

Lukas Nellen

List of Publications by Year in descending order

Source: <https://exaly.com/author-pdf/7688552/publications.pdf>

Version: 2024-02-01

437
papers

24,431
citations

9786
73
h-index

9589
142
g-index

447
all docs

447
docs citations

447
times ranked

13998
citing authors

#	ARTICLE	IF	CITATIONS
1	Multi-messenger Observations of a Binary Neutron Star Merger [*] . <i>Astrophysical Journal Letters</i> , 2017, 848, L12.	8.3	2,805
2	The ALICE experiment at the CERN LHC. <i>Journal of Instrumentation</i> , 2008, 3, S08002-S08002.	1.2	811
3	Multimessenger observations of a flaring blazar coincident with high-energy neutrino IceCube-170922A. <i>Science</i> , 2018, 361, .	12.6	654
4	Properties and performance of the prototype instrument for the Pierre Auger Observatory. <i>Nuclear Instruments and Methods in Physics Research, Section A: Accelerators, Spectrometers, Detectors and Associated Equipment</i> , 2004, 523, 50-95.	1.6	647
5	Correlation of the Highest-Energy Cosmic Rays with Nearby Extragalactic Objects. <i>Science</i> , 2007, 318, 938-943.	12.6	647
6	Introducing the CTA concept. <i>Astroparticle Physics</i> , 2013, 43, 3-18.	4.3	504
7	Observation of the Suppression of the Flux of Cosmic Rays above mml:math $\text{display="inline"}>\langle \text{mml:mn} \rangle 4 \langle /mml:mn \rangle \langle \text{mml:mo} \rangle \text{--} \langle /mml:mo \rangle \langle \text{mml:msup} \rangle \langle \text{mml:mn} \rangle 10 \langle /mml:mn \rangle \langle \text{mml:mn} \rangle 7.8 \langle /mml:mn \rangle \langle \text{mml:msup} \rangle \langle \text{mml:mn} \rangle 500 \langle /mml:mn \rangle \langle \text{mml:mo} \rangle \text{--} \langle /mml:mo \rangle \langle \text{mml:msup} \rangle \langle \text{mml:mn} \rangle 10 \langle /mml:mn \rangle \langle \text{mml:mn} \rangle 7.8 \langle /mml:mn \rangle \langle \text{mml:msup} \rangle \langle \text{mml:mn} \rangle 500 \langle /mml:mn \rangle$ Physical Review Letters, 2008, 101, 061101.		
8	The Pierre Auger Cosmic Ray Observatory. <i>Nuclear Instruments and Methods in Physics Research, Section A: Accelerators, Spectrometers, Detectors and Associated Equipment</i> , 2015, 798, 172-213.	1.6	442
9	ALICE: Physics Performance Report, Volume II. <i>Journal of Physics G: Nuclear and Particle Physics</i> , 2006, 32, 1295-2040.	3.6	441
10	Measurement of the Depth of Maximum of Extensive Air Showers above mml:math $\text{display="block"}>\langle \text{mml:msup} \rangle \langle \text{mml:mn} \rangle 10 \langle /mml:mn \rangle \langle \text{mml:mn} \rangle 18 \langle /mml:mn \rangle \langle \text{mml:msup} \rangle \langle \text{mml:mtext} \rangle \text{--} \langle /mml:mtext \rangle \langle \text{mml:msup} \rangle \langle \text{mml:mn} \rangle 7.8 \langle /mml:mn \rangle \langle \text{mml:msup} \rangle \langle \text{mml:mn} \rangle 429 \langle /mml:mn \rangle$ Physical Review Letters, 2010, 104, 091101.		
11	Enhanced production of multi-strange hadrons in high-multiplicity protonâ“proton collisions. <i>Nature Physics</i> , 2017, 13, 535-539.	16.7	399
12	Measurement of the energy spectrum of cosmic rays above 10 ¹⁸ eV using the Pierre Auger Observatory. <i>Physics Letters, Section B: Nuclear, Elementary Particle and High-Energy Physics</i> , 2010, 685, 239-246.	4.1	357
13	Extended gamma-ray sources around pulsars constrain the origin of the positron flux at Earth. <i>Science</i> , 2017, 358, 911-914.	12.6	303
14	The fluorescence detector of the Pierre Auger Observatory. <i>Nuclear Instruments and Methods in Physics Research, Section A: Accelerators, Spectrometers, Detectors and Associated Equipment</i> , 2010, 620, 227-251.	1.6	275
15	Update on the correlation of the highest energy cosmic rays with nearby extragalactic matter. <i>Astroparticle Physics</i> , 2010, 34, 314-326.	4.3	270
16	Depth of maximum of air-shower profiles at the Pierre Auger Observatory. I. Measurements at energies above mml:math $\text{display="block"}>\langle \text{mml:mrow} \rangle \langle \text{mml:mn} \rangle 1 \langle /mml:mn \rangle \langle \text{mml:msup} \rangle \langle \text{mml:mrow} \rangle \langle \text{mml:mn} \rangle 0 \langle /mml:mn \rangle \langle \text{mml:mrow} \rangle \langle \text{mml:mn} \rangle 4.7 \langle /mml:mn \rangle \langle \text{mml:mrow} \rangle \langle \text{mml:mn} \rangle 266 \langle /mml:mn \rangle$ Physical Review D, 2014, 90, .		
17	Observation of a large-scale anisotropy in the arrival directions of cosmic rays above 8 Å– 10 ¹⁸ eV. <i>Science</i> , 2017, 357, 1266-1270.	12.6	261
18	Depth of maximum of air-shower profiles at the Pierre Auger Observatory. II. Composition implications. <i>Physical Review D</i> , 2014, 90, .	4.7	213

#	ARTICLE	IF	CITATIONS
19	Measurement of the Proton-Air Cross Section at $\sqrt{s} = 57 \text{ TeV}$ at the Pierre Auger Observatory. <i>Physical Review Letters</i> , 2012, 109, 062002.	7.8	212
20	The 2HWC HAWC Observatory Gamma-Ray Catalog. <i>Astrophysical Journal</i> , 2017, 843, 40.	4.5	200
21	Combined fit of spectrum and composition data as measured by the Pierre Auger Observatory. <i>Journal of Cosmology and Astroparticle Physics</i> , 2017, 2017, 038-038.	5.4	191
22	Centrality Dependence of the Charged-Particle Multiplicity Density at Midrapidity in Pb-Pb Collisions at $\sqrt{s} = 2.76 \text{ TeV}$. <i>Physical Review Letters</i> , 2016, 116, 222302.	7.8	182
23	An Indication of Anisotropy in Arrival Directions of Ultra-high-energy Cosmic Rays through Comparison to the Flux Pattern of Extragalactic Gamma-Ray Sources γ . <i>Astrophysical Journal Letters</i> , 2018, 853, L29.	8.3	165
24	Direct photon production in Pb-Pb collisions at $\sqrt{s} = 2.76 \text{ TeV}$. <i>Nuclear Physics Letters, Section B: Nuclear, Elementary Particle and High-Energy Physics</i> , 2016, 754, 235-248.	1.1	163
25	Upper limit on the cosmic-ray photon flux above 10^{19} eV using the surface detector of the Pierre Auger Observatory. <i>Astroparticle Physics</i> , 2008, 29, 243-256.	4.3	161
26	Observation of the Crab Nebula with the HAWC Gamma-Ray Observatory. <i>Astrophysical Journal</i> , 2017, 843, 39.	4.5	159
27	Sensitivity of the high altitude water Cherenkov detector to sources of multi-TeV gamma rays. <i>Astroparticle Physics</i> , 2013, 50-52, 26-32.	4.3	156
28	Testing Hadronic Interactions at Ultrahigh Energies with Air Showers Measured by the Pierre Auger Observatory. <i>Physical Review Letters</i> , 2016, 117, 192001.	7.8	154
29	Muons in air showers at the Pierre Auger Observatory: Mean number in highly inclined events. <i>Physical Review D</i> , 2015, 91, 1.	4.7	152
30	Trigger and aperture of the surface detector array of the Pierre Auger Observatory. <i>Nuclear Instruments and Methods in Physics Research, Section A: Accelerators, Spectrometers, Detectors and Associated Equipment</i> , 2010, 613, 29-39.	1.6	151
31	Measurement of pion, kaon and proton production in proton-proton collisions at $\sqrt{s} = 7 \text{ TeV}$. <i>European Physical Journal C</i> , 2015, 75, 226.	3.9	149
32	Anisotropic Flow of Charged Particles in Pb-Pb Collisions at $\sqrt{s} = 2.76 \text{ TeV}$. <i>Physical Review Letters</i> , 2016, 116, 132302.	7.8	148
33	SEARCHES FOR ANISOTROPIES IN THE ARRIVAL DIRECTIONS OF THE HIGHEST ENERGY COSMIC RAYS DETECTED BY THE PIERRE AUGER OBSERVATORY. <i>Astrophysical Journal</i> , 2015, 804, 15.	4.5	146
34	Multiple Galactic Sources with Emission Above 56 TeV Detected by HAWC. <i>Physical Review Letters</i> , 2020, 124, 021102.	7.8	143
35	Upper Limit on the Diffuse Flux of Ultrahigh Energy Tau Neutrinos from the Pierre Auger Observatory. <i>Physical Review Letters</i> , 2008, 100, 211101.	7.8	141
36	Correlated Event-by-Event Fluctuations of Flow Harmonics in Pb-Pb Collisions at $\sqrt{s} = 2.76 \text{ TeV}$. <i>Physical Review Letters</i> , 2016, 117, 182301.	7.8	138

#	ARTICLE	IF	CITATIONS
37	Multiplicity dependence of particle production in Pb-Pb collisions at $\sqrt{s_{\text{NN}}} = 2.76 \text{ TeV}$. Physical Review C, 2015, 91, 054902.	8.3	135
38	Search for High-energy Neutrinos from Binary Neutron Star Merger GW170817 with ANTARES, IceCube, and the Pierre Auger Observatory. Astrophysical Journal Letters, 2017, 850, L35.	8.3	135
39	Production of light nuclei and anti-nuclei in pp and Pb-Pb collisions at energies available at the CERN Large Hadron Collider. Physical Review C, 2016, 93, 054902.	2.9	129
40	Improved limit to the diffuse flux of ultrahigh energy neutrinos from the Pierre Auger Observatory. Physical Review D, 2015, 91, 093005.	4.7	125
41	The offline software framework of the Pierre Auger Observatory. Nuclear Instruments and Methods in Physics Research, Section A: Accelerators, Spectrometers, Detectors and Associated Equipment, 2007, 580, 1485-1496.	1.6	120
42	Upper limit on the cosmic-ray photon fraction at EeV energies from the Pierre Auger Observatory. Astroparticle Physics, 2009, 31, 399-406.	4.3	117
43	Multi-strange baryon production in p-Pb collisions at $\sqrt{s_{\text{NN}}} = 2.76 \text{ TeV}$. Physics Letters, Section B: Nuclear, Elementary Particle and High-Energy Physics, 2016, 758, 389-401.	111	111
44	On the sensitivity of the HAWC observatory to gamma-ray bursts. Astroparticle Physics, 2012, 35, 641-650.	4.3	100
45	Limit on the diffuse flux of ultrahigh energy tau neutrinos with the surface detector of the Pierre Auger Observatory. Physical Review D, 2009, 79, 093005.	4.7	99
46	3HWC: The Third HAWC Catalog of Very-high-energy Gamma-Ray Sources. Astrophysical Journal, 2020, 905, 76.	4.5	99
47	Measurement of the Crab Nebula Spectrum Past 100 TeV with HAWC. Astrophysical Journal, 2019, 881, 134.	4.5	98
48	Measurement of the cosmic-ray energy spectrum above 10^{19} eV using the Pierre Auger Observatory. Physical Review D, 2020, 102, 093005.	4.7	97
49	Transverse momentum spectra and nuclear modification factors of charged particles in pp , p-Pb and Pb-Pb collisions at the LHC. Journal of High Energy Physics, 2018, 2018, 1.	4.7	97
50	Antennas for the detection of radio emission pulses from cosmic-ray induced air showers at the Pierre Auger Observatory. Journal of Instrumentation, 2012, 7, P10011-P10011.	1.2	95
51	Multiplicity dependence of charged pion, kaon, and (anti)proton production at large transverse momentum in p-Pb collisions at $\sqrt{s_{\text{NN}}} = 2.76 \text{ TeV}$. Physics Letters, Section B: Nuclear, Elementary Particle and High-Energy Physics, 2016, 760, 720-735.	4.1	93
52	Suppression at forward rapidity in Pb-Pb collisions at $\sqrt{s_{\text{NN}}} = 2.76 \text{ TeV}$. Physics Letters, Section B: Nuclear, Elementary Particle and High-Energy Physics, 2017, 766, 212-224.	1.1	92

#	ARTICLE	IF	CITATIONS
55	Measurement of the Radiation Energy in the Radio Signal of Extensive Air Showers as a Universal Estimator of Cosmic-Ray Energy. <i>Physical Review Letters</i> , 2016, 116, 241101.	7.8	91
56	An upper limit to the photon fraction in cosmic rays above 10^{19} eV from the Pierre Auger Observatory. <i>Astroparticle Physics</i> , 2007, 27, 155-168.	4.3	90
57	Production of K^{*0} and $\phi(1020)$ in $p\bar{p}$ collisions at $\sqrt{s_{NN}} = 5.02$ TeV. <i>European Physical Journal C</i> , 2016, 76, 245.	3.9	89
58	Multiplicity dependence of light-flavor hadron production in $p\bar{p}$ collisions at $\sqrt{s_{NN}} = 5.02$ TeV. <i>Physical Review C</i> , 2019, 99, 1.	2.9	89
59	Transverse momentum dependence of D-meson production in Pb-Pb collisions at $\sqrt{s_{NN}} = 2.76$ TeV. <i>Journal of High Energy Physics</i> , 2016, 2016, 1.	4.7	88
60	Centrality dependence of the nuclear modification factor of charged pions, kaons, and protons in Pb-Pb collisions at $\sqrt{s_{NN}} = 2.76$ TeV. <i>Physical Review C</i> , 2016, 93, 1.	4.7	87
61	and meson production at high transverse momentum in $p\bar{p}$. <i>Physical Review C</i> , 2017, 95, 1.	2.9	86
62	Probing the radio emission from air showers with polarization measurements. <i>Physical Review D</i> , 2014, 89, 1.	4.7	85
63	A study of the effect of molecular and aerosol conditions in the atmosphere on air fluorescence measurements at the Pierre Auger Observatory. <i>Astroparticle Physics</i> , 2010, 33, 108-129.	4.3	84
64	Evidence for a mixed mass composition at the ankle in the cosmic-ray spectrum. <i>Physics Letters, Section B: Nuclear, Elementary Particle and High-Energy Physics</i> , 2016, 762, 288-295.	4.1	84
65	Pseudorapidity and transverse-momentum distributions of charged particles in proton-proton collisions at $\sqrt{s} = 13$ TeV. <i>Physics Letters, Section B: Nuclear, Elementary Particle and High-Energy Physics</i> , 2016, 753, 319-329.	4.1	82
66	Inferences on mass composition and tests of hadronic interactions from 0.3 to 100 GeV using the water-Cherenkov detectors of the Pierre Auger Observatory. <i>Physical Review D</i> , 2017, 96, 1.	4.7	82
67	Energy estimation of cosmic rays with the Engineering Radio Array of the Pierre Auger Observatory. <i>Physical Review D</i> , 2016, 93, 1.	4.7	80
68	-Meson Azimuthal Anisotropy in Midcentral Pb-Pb Collisions at $\sqrt{s_{NN}} = 5.02$ TeV. <i>Physical Review Letters</i> , 2016, 117, 122301.	7.8	80
69	Features of the Energy Spectrum of Cosmic Rays above 10^{19} eV. <i>Using the Pierre Auger Observatory</i> . <i>Physical Review Letters</i> , 2020, 125, 121106.	7.8	79
70	Measurement of an Excess in the Yield of π^+ and π^- at Very Low η . <i>Nature</i> , 2018, 558, 541-544.	7.8	77
71	Large-scale Cosmic-Ray Anisotropies above 4 EeV Measured by the Pierre Auger Observatory. <i>Astrophysical Journal</i> , 2018, 868, 4.	4.5	77
72	Very-high-energy particle acceleration powered by the jets of the microquasar SS 433. <i>Nature</i> , 2018, 562, 82-85.	27.8	75

#	ARTICLE	IF	CITATIONS
91	Charged-particle multiplicities in proton–proton collisions at $\sqrt{s} = 0.9$ to 8 TeV. European Physical Journal C, 2017, 77, 1.	3.9	62
92	Measurement of D-meson production at mid-rapidity in pp collisions at $\sqrt{s} = 7$ TeV. European Physical Journal C, 2017, 77, 1.	3.9	62
93	Centrality and pseudorapidity dependence of the charged-particle multiplicity density in $\text{Xe} + \text{Xe}$ collisions at $\sqrt{s_{\text{NN}}} = 2.76$ TeV. Physics Letters, Section B: Nuclear, Elementary Particle and High-Energy Physics, 2019, 790, 35-48.	4.1	62
94	HAWC observations of the acceleration of very-high-energy cosmic rays in the Cygnus Cocoon. Nature Astronomy, 2021, 5, 465-471.	10.1	62
95	All-particle cosmic ray energy spectrum measured by the HAWC experiment from 10 to 500 TeV. Physical Review D, 2017, 96, .	4.7	56
96	Constraining the magnitude of the Chiral Magnetic Effect with Event Shape Engineering in Pb+Pb collisions at $\sqrt{s_{\text{NN}}} = 5.02$ and 2.76 TeV. Physics Letters, Section B: Nuclear, Elementary Particle and High-Energy Physics, 2018, 777, 151-162.	4.0	56
97	SEARCH FOR POINT-LIKE SOURCES OF ULTRA-HIGH ENERGY NEUTRINOS AT THE PIERRE AUGER OBSERVATORY AND IMPROVED LIMIT ON THE DIFFUSE FLUX OF TAU NEUTRINOS. Astrophysical Journal Letters, 2012, 755, L4.	8.3	55
98	Energy dependence and fluctuations of anisotropic flow in Pb-Pb collisions at $\sqrt{s_{\text{NN}}} = 5.02$ and 2.76 TeV. Journal of High Energy Physics, 2018, 2018, 1.	4.7	55
99	The exposure of the hybrid detector of the Pierre Auger Observatory. Astroparticle Physics, 2011, 34, 368-381.	4.3	54
100	Measurement of D0, D+, D*+ and D+s production in Pb-Pb collisions at $\sqrt{s_{\text{NN}}} = 5.02$ TeV. Journal of High Energy Physics, 2018, 2018, 1.	4.7	54
101	Advanced functionality for radio analysis in the Offline software framework of the Pierre Auger Observatory. Nuclear Instruments and Methods in Physics Research, Section A: Accelerators, Spectrometers, Detectors and Associated Equipment, 2011, 635, 92-102.	1.6	52
102	Anisotropy studies around the galactic centre at EeV energies with the Auger Observatory. Astroparticle Physics, 2007, 27, 244-253.	4.3	51
103	Search for ultrahigh energy neutrinos in highly inclined events at the Pierre Auger Observatory. Physical Review D, 2011, 84, .	4.7	51
104	Measurement of charm and beauty production at central rapidity versus charged-particle multiplicity in proton-proton collisions at $s = 7$ TeV. Journal of High Energy Physics, 2015, 2015, 1.	4.7	50
105	Linear and non-linear flow mode in Pb+Pb collisions at $\sqrt{s_{\text{NN}}} = 2.76$ TeV. Physics Letters, Section B: Nuclear, Elementary Particle and High-Energy Physics, 2017, 779, 68-80.	5.1	50
106	Energy dependence of forward-rapidity $\psi(0)$ and $\psi(2S)$ production in pp collisions at the LHC. European Physical Journal C, 2017, 77, 392.	3.9	50
107	Reconstruction of inclined air showers detected with the Pierre Auger Observatory. Journal of Cosmology and Astroparticle Physics, 2014, 2014, 019-019.	5.4	49
108	Measurement of charged jet production cross sections and nuclear modification in Pb+Pb collisions at $\sqrt{s_{\text{NN}}} = 2.76$ TeV. Physics Letters, Section B: Nuclear, Elementary Particle and High-Energy Physics, 2015, 749, 68-81.	5.1	49

#	ARTICLE	IF	CITATIONS
109	LARGE SCALE DISTRIBUTION OF ULTRA HIGH ENERGY COSMIC RAYS DETECTED AT THE PIERRE AUGER OBSERVATORY WITH ZENITH ANGLES UP TO 80°. <i>Astrophysical Journal</i> , 2015, 802, 111.	4.5	49
110	Search for photons with energies above 10^{18} eV using the hybrid detector of the Pierre Auger Observatory. <i>Journal of Cosmology and Astroparticle Physics</i> , 2017, 2017, 009-009.	5.4	49
111	Charged-particle production as a function of multiplicity and transverse spherocity in pp collisions at $\sqrt{s} = 5.02$ and 13 TeV. <i>European Physical Journal C</i> , 2019, 79, 1.	3.9	49
112	Multiplicity dependence of (multi-)strange hadron production in proton-proton collisions at $\sqrt{s} = 13$ TeV. <i>European Physical Journal C</i> , 2020, 80, 1.	3.9	49
113	Measurement of jet quenching with semi-inclusive hadron-jet distributions in central Pb-Pb collisions at $s_{NN} = 2.76$ TeV. <i>Journal of High Energy Physics</i> , 2015, 2015, 1.	4.7	48
114	HAWC J2227+610 and Its Association with G106.3+2.7, a New Potential Galactic PeVatron. <i>Astrophysical Journal Letters</i> , 2020, 896, L29.	8.3	48
115	production in $\sqrt{s} = 5.02$ and 13 TeV. <i>European Physical Journal C</i> , 2019, 79, 47	2.9	47
116	One-dimensional pion, kaon, and proton femtoscopy in Pb-Pb collisions at $\sqrt{s} = 2.76$ TeV. <i>Physical Review C</i> , 2015, 92, 054906.	2.9	46
117	Forward-central two-particle correlations in $\sqrt{s} = 5.02$ and 13 TeV. <i>Journal of High Energy Physics</i> , 2016, 753, 126-139.	4.1	45
118	Elliptic Flow in Pb-Pb Collisions at $\sqrt{s} = 2.76$ TeV. <i>Physical Review Letters</i> , 2017, 119, 242301.	7.8	45
119	LARGE-SCALE DISTRIBUTION OF ARRIVAL DIRECTIONS OF COSMIC RAYS DETECTED ABOVE 10^{18} eV AT THE PIERRE AUGER OBSERVATORY. <i>Astrophysical Journal Supplement Series</i> , 2012, 203, 34.	7.7	44
120	Determination of the event collision time with the ALICE detector at the LHC. <i>European Physical Journal Plus</i> , 2017, 132, 1.	2.6	44
121	The energy spectrum of cosmic rays beyond the turn-down around $\sqrt{s} = 10^{17}$ TeV as measured with the surface detector of the Pierre Auger Observatory. <i>European Physical Journal C</i> , 2021, 81, 1.	3.9	44
122	Atmospheric effects on extensive air showers observed with the surface detector of the Pierre Auger observatory. <i>Astroparticle Physics</i> , 2009, 32, 89-99.	4.3	43
123	Charge-dependent flow and the search for the chiral magnetic wave in Pb-Pb collisions at $\sqrt{s} = 2.76$ TeV. <i>Physical Review C</i> , 2016, 93, 054906.	4.0	43
124	Measurement of $\Lambda_c^0 \rightarrow \Lambda_c^+ + \pi^-$ production in pp collisions at $\sqrt{s} = 5.02$ TeV with ALICE. <i>European Physical Journal C</i> , 2019, 79, 1.	3.9	43
125	$\bar{b} + c$ production in pp collisions at $\sqrt{s} = 7$ TeV and in p-Pb collisions at $\sqrt{s} = 5.02$ TeV. <i>Journal of High Energy Physics</i> , 2018, 2018, 1.	4.7	42
126	Precision measurement of the mass difference between light nuclei and anti-nuclei. <i>Nature Physics</i> , 2015, 11, 811-814.	16.7	41

#	ARTICLE	IF	CITATIONS
127	Higher harmonic flow coefficients of identified hadrons in Pb-Pb collisions at $s_{NN} = 2.76 \text{ TeV}$. Journal of High Energy Physics, 2016, 2016, 1.	4.7	40
128	Centrality evolution of the charged-particle pseudorapidity density over a broad pseudorapidity range in Pb-Pb collisions at $\sqrt{s_{NN}} = 2.76 \text{ TeV}$. Journal of High Energy Physics Letters, Section B: Nuclear, Elementary Particle and High-Energy Physics, 2016, 754, 373-385.	4.0	40
129	Measurement of deuteron spectra and elliptic flow in Pb-Pb collisions at $\sqrt{s_{NN}} = 2.76 \text{ TeV}$ at the LHC. European Physical Journal C, 2017, 77, 1.	3.9	40
130	Anisotropic flow of identified particles in Pb-Pb collisions at $\sqrt{s_{NN}} = 5.02 \text{ TeV}$. Journal of High Energy Physics, 2018, 2018, 1.	4.7	40
131	Constraints on Lorentz Invariance Violation from HAWC Observations of Gamma Rays above 100 TeV . Physical Review Letters, 2020, 124, 131101.	7.8	40
132	Ultrahigh Energy Neutrinos at the Pierre Auger Observatory. Advances in High Energy Physics, 2013, 2013, 1-18.	1.1	39
133	Two-pion femtoscopy in Pb-Pb collisions at $\sqrt{s_{NN}} = 2.76 \text{ TeV}$. Physical Review C, 2015, 91, 014902.	2.9	39
134	Inclusive quarkonium production at forward rapidity in pp collisions at $\sqrt{s} = 8 \text{ TeV}$. European Physical Journal C, 2016, 76, 184.	3.9	39
135	Daily Monitoring of TeV Gamma-Ray Emission from Mrk 421, Mrk 501, and the Crab Nebula with HAWC. Astrophysical Journal, 2017, 841, 100.	4.5	39
136	First measurement of jet mass in Pb-Pb and p-Pb collisions at the LHC. Physics Letters, Section B: Nuclear, Elementary Particle and High-Energy Physics, 2018, 776, 249-264.	4.1	39
137	Coherent π^0 photo-production in ultra-peripheral Pb-Pb collisions at $\sqrt{s_{NN}} = 2.76 \text{ TeV}$. Physics Letters, Section B: Nuclear, Elementary Particle and High-Energy Physics, 2015, 751, 358-370.	3.8	39
138	Cosmic-Ray Anisotropies in Right Ascension Measured by the Pierre Auger Observatory. Astrophysical Journal, 2020, 891, 142.	4.5	39
139	Sensitivity of HAWC to high-mass dark matter annihilations. Physical Review D, 2014, 90, .	4.7	38
140	Coherent π^0 photo-production in ultra-peripheral Pb-Pb collisions at $\sqrt{s_{NN}} = 2.76 \text{ TeV}$. Physics Letters, Section B: Nuclear, Elementary Particle and High-Energy Physics, 2015, 751, 358-370.	3.8	38
141	Rapidity and transverse-momentum dependence of the inclusive J/ψ nuclear modification factor in p-Pb collisions at $\sqrt{s_{NN}} = 5.02 \text{ TeV}$. Journal of High Energy Physics, 2015, 2015, 1.	4.7	38
142	Ultrahigh-energy neutrino follow-up of gravitational wave events GW150914 and GW151226 with the Pierre Auger Observatory. Physical Review D, 2016, 94, .	4.7	38
143	Prototype muon detectors for the AMIGA component of the Pierre Auger Observatory. Journal of Instrumentation, 2016, 11, P02012-P02012.	1.2	38
144	Measurement of $\langle \cos(\Delta\phi) \rangle$ in Pb-Pb collisions at $\sqrt{s_{NN}} = 2.76 \text{ TeV}$. Physics Letters, Section B: Nuclear, Elementary Particle and High-Energy Physics, 2017, 767, 10-16.	7.8	38

#	ARTICLE	IF	CITATIONS
145	Multiplicity dependence of π , K, and p production in pp collisions at $\sqrt{s} = 13 \text{ TeV}$. Evidence of rescattering effect in Pb-Pb collisions at the LHC through production of K . European Physical Journal C, 2020, 80, 1.	3.9	38
146	$\text{altimg} = "si1.svg" < \text{mml:multiscripts} > \text{mml:mrow} < \text{mml:mo} \text{stretchy} = "false" > (< \text{mml:mo} > 892 < \text{mml:mn} > < \text{mml:mo} > \text{Tj ETQq0 0 0 rgBT /Overlock 10 Tf 50 697 Td (stretchy} = "false" >) < \text{mml:mn} > 0 < \text{mml:mn} > < \text{mml:mrow} > < \text{mml:mprescripts} /> < \text{mml:none} /> < \text{mml:mrow} > \text{mml:mi} < \text{mml:msub} > < \text{mml:mrow} > < \text{mml:mi} > s < \text{mml:mi} > < \text{mml:mrow} > < \text{mml:mi} > \text{mathvariant} = "normal" > NN < \text{mml:mi} > < \text{mml:mrow} > < \text{mml:msub} > < \text{mml:mrow} > < \text{mml:msqrt} > < \text{mml:mspace width} = "0.25em" /> < \text{mml:mo} \text{linebreak} = "goodbreak" \text{linebreakstyle} = "after" > = < \text{mml:mo} > < \text{mml:mspace width} = "0.25em" /> < \text{mml:mn} > 5.02 < \text{mml:mn} > < \text{mml:math} > \text{TeV}$. Physics Letters, Section B: Nuclear, Elementary Particle and High-Energy Physics, 1991, 261, 441-473.	2.5	37
147	Half-string oscillator approach to string field theory. Nuclear Physics B, 1991, 351, 441-473.	2.5	37
148	Yukawa couplings for the spinning particle and the world-line formalism. Physics Letters, Section B: Nuclear, Elementary Particle and High-Energy Physics, 1995, 351, 200-205.	4.1	37
149	Constraints on spin-dependent dark matter scattering with long-lived mediators from TeV observations of the Sun with HAWC. Physical Review D, 2018, 98.	4.7	37
150	$\text{mathvariant} = "normal" > NN < \text{mml:mi} > < \text{mml:mrow} > < \text{mml:msub} > < \text{mml:mrow} > < \text{mml:mi} > \text{width} = "0.25em" /> < \text{mml:mo} \text{linebreak} = "goodbreak" \text{linebreakstyle} = "after" > = < \text{mml:mo} > < \text{mml:mspace width} = "0.25em" /> < \text{mml:mn} > 5.02 < \text{mml:mn} > < \text{mml:math} > \text{TeV}$. Physics Letters, Section B: Nuclear, Elementary Particle and High-Energy Physics, 2015, 2015, 1.	4.1	37
151	Forward-backward multiplicity correlations in pp collisions at $s = \sqrt{s} = 0.9, 2.76$ and 7 TeV . Journal of High Energy Physics, 2015, 2015, 1.	4.7	36
152	Measurement of transverse energy at midrapidity in Pb-Pb collisions at $\sqrt{s} = 2.76 \text{ TeV}$. Physical Review C, 2016, 94.	4.7	36
153	Centrality dependence of pion freeze-out radii in Pb-Pb collisions at $\sqrt{s} = 2.76 \text{ TeV}$. Physical Review C, 2016, 93.	4.7	36
154	Production of $\Sigma(1385)^{\pm}$. European Physical Journal C, 2017, 77, 389.	3.9	36
155	A search for dark matter in the Galactic halo with HAWC. Journal of Cosmology and Astroparticle Physics, 2018, 2018, 049-049.	5.4	36
156	Direct measurement of the muonic content of extensive air showers between $2 \times 10^{17} \text{ eV}$ and $2 \times 10^{18} \text{ eV}$ at the Pierre Auger Observatory. European Physical Journal C, 2020, 80, 1.	3.9	36
157	Centrality dependence of high-pT D meson suppression in Pb-Pb collisions at $s = 2.76 \text{ TeV}$. Journal of High Energy Physics, 2015, 2015, 1.	4.7	35
158	Direct photon elliptic flow in Pb-Pb collisions at $\sqrt{s} = 2.76 \text{ TeV}$. Physics Letters, Section B: Nuclear, Elementary Particle and High-Energy Physics, 2019, 789, 308-322.	4.7	35
159	Measurement of the cosmic ray energy spectrum using hybrid events of the Pierre Auger Observatory. European Physical Journal Plus, 2012, 127, 1.	2.6	34
160	Bounds on the density of sources of ultra-high energy cosmic rays from the Pierre Auger Observatory. Journal of Cosmology and Astroparticle Physics, 2013, 2013, 009-009.	5.4	34
161	$\pi^0 \text{ and } \eta \text{ meson production in proton-proton collisions at } \sqrt{s} = 8 \text{ TeV}$. European Physical Journal C, 2018, 78, 1.	3.9	34
162	$\text{mathvariant} = "normal" > H < \text{mml:mi} > < \text{mml:mrow} > < \text{mml:mprescripts} /> < \text{mml:mrow} > < \text{mml:mi} > \text{mathvariant} = "normal" > \bar{p} < \text{mml:mi} > < \text{mml:mrow} > < \text{mml:msub} > < \text{mml:mrow} > < \text{mml:mi} > 3 < \text{mml:mi} > < \text{mml:mrow} > < \text{mml:msub} > < \text{mml:mrow} > < \text{mml:msqrt} > < \text{mml:mo} > = < \text{mml:mo} > < \text{mml:mspace width} = "0.25em" /> < \text{mml:mo} > < \text{mml:mspace width} = "0.25em" /> < \text{mml:mn} > m < \text{mml:mn} > < \text{mml:math} > \text{and}$. European Physical Journal C, 2018, 78, 1.	3.9	34

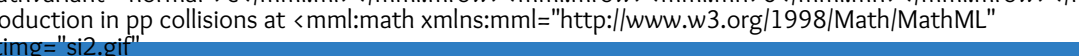
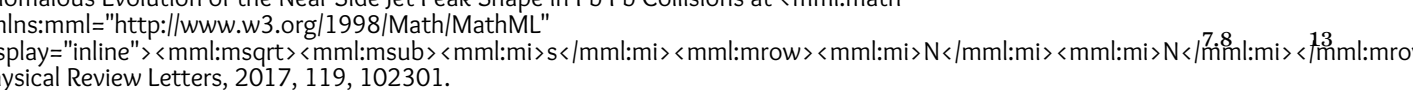
#	ARTICLE	IF	CITATIONS
163	Energy dependence of exclusive J/ψ photoproduction off protons in ultra-peripheral $\mathrm{p}+\mathrm{Pb}$ collisions at $\sqrt{s_{\mathrm{NN}}} = 5.02 \text{ TeV}$. European Physical Journal C, 2019, 79, 1.	3.9	34
164	Evidence of 200 TeV Photons from HAWC J1825-134. Astrophysical Journal Letters, 2021, 907, L30.	8.3	34
165	Measurement of the Fluctuations in the Number of Muons in Extensive Air Showers with the Pierre Auger Observatory. Physical Review Letters, 2021, 126, 152002.	7.8	34
166	SEARCH FOR TeV GAMMA-RAY EMISSION FROM POINT-LIKE SOURCES IN THE INNER GALACTIC PLANE WITH A PARTIAL CONFIGURATION OF THE HAWC OBSERVATORY. Astrophysical Journal, 2016, 817, 3.	4.5	33
167	Differential studies of inclusive J/ψ and $\psi(2S)$ production at forward rapidity in Pb-Pb collisions at $s_{\mathrm{NN}} = 2.76 \text{ TeV}$. Journal of High Energy Physics, 2016, 2016, 1. Measurement of electrons from heavy-flavour hadron decays in $\mathrm{p}+\mathrm{Pb}$ collisions at $\sqrt{s_{\mathrm{NN}}} = 5.02 \text{ TeV}$. Physics Letters, Section B: Nuclear, Elementary Particle and High-Energy Physics, 2016, 754, 81-93.	4.7	33
168	$\mathrm{NN} < \mathrm{mml:mi} < \mathrm{mml:mrow} < \mathrm{mml:msub} < \mathrm{mml:mi} < \mathrm{mml:mi} < \mathrm{mml:mrow} < \mathrm{mml:mo} < \mathrm{mml:mn} < \mathrm{mml:mi} < \mathrm{mml:msqrt} < \mathrm{mml:mo} < \mathrm{mml:mn} < \mathrm{mml:mi} < \mathrm{mml:mtext} < \mathrm{mml:mo} < \mathrm{mml:mn} < \mathrm{mml:mi} < \mathrm{mml:mtext} < \mathrm{mml:math}$. Physics Letters, Section B: Nuclear, Elementary Particle and High-Energy Physics, 2016, 754, 81-93.	4.7	33
169	Multiwavelength follow-up of a rare IceCube neutrino multiplet. Astronomy and Astrophysics, 2017, 607, A115.	5.1	33
170	Axial couplings on the world-line. Physics Letters, Section B: Nuclear, Elementary Particle and High-Energy Physics, 1996, 366, 212-219.	4.1	32
171	Search for signatures of magnetically-induced alignment in the arrival directions measured by the Pierre Auger Observatory. Astroparticle Physics, 2012, 35, 354-361.	4.3	32
172	Charged-particle multiplicity distributions over a wide pseudorapidity range in proton-proton collisions at $\sqrt{s} = 0.9, 7, \text{ and } 8 \text{ TeV}$. European Physical Journal C, 2017, 77, 1.	3.9	32
173	All-sky Measurement of the Anisotropy of Cosmic Rays at 10 TeV and Mapping of the Local Interstellar Magnetic Field. Astrophysical Journal, 2019, 871, 96.	4.5	32
174	Evidence that Ultra-high-energy Gamma Rays Are a Universal Feature near Powerful Pulsars. Astrophysical Journal Letters, 2021, 911, L27.	8.3	32
175	Centrality dependence of charged jet production in $\mathrm{p}+\mathrm{Pb}$ collisions at $\sqrt{s_{\mathrm{NN}}} = 5.02 \text{ TeV}$. European Physical Journal C, 2016, 76, 271.	3.9	31
176	Search for correlations between the arrival directions of IceCube neutrino events and ultrahigh-energy cosmic rays detected by the Pierre Auger Observatory and the Telescope Array. Journal of Cosmology and Astroparticle Physics, 2016, 2016, 037-037.	5.4	31
177	Insight into particle production mechanisms via angular correlations of identified particles in pp collisions at $\sqrt{s} = 7 \text{ TeV}$. European Physical Journal C, 2017, 77, 1.	3.9	31
178	Neutral pion and η -meson production in $\mathrm{p}+\mathrm{Pb}$ collisions at $\sqrt{s_{\mathrm{NN}}} = 5.02 \text{ TeV}$. European Physical Journal C, 2018, 78, 1.	3.9	31
179	Inclusive, prompt and non-prompt J/ψ production at mid-rapidity in Pb-Pb collisions at $s_{\mathrm{NN}} = 2.76 \text{ TeV}$. Journal of High Energy Physics, 2015, 2015, 1.	4.7	30
180	Coherent J/ψ photoproduction in ultra-peripheral Pb-Pb collisions at $s_{\mathrm{NN}} = 2.76 \text{ TeV}$. Journal of High Energy Physics, 2015, 2015, 1.	4.7	30

#	ARTICLE	IF	CITATIONS
181	SEARCH FOR GAMMA-RAYS FROM THE UNUSUALLY BRIGHT GRB 130427A WITH THE HAWC GAMMA-RAY OBSERVATORY. <i>Astrophysical Journal</i> , 2015, 800, 78.	4.5	30
182	Multiplicity and transverse momentum evolution of charge-dependent correlations in pp, p+Pb, and Pb+Pb collisions at the LHC. <i>European Physical Journal C</i> , 2016, 76, 86.	3.9	30
183	Pseudorapidity dependence of the anisotropic flow of charged particles in Pb+Pb collisions at $\sqrt{s_{NN}} = 2.76 \text{ TeV}$. <i>Physics Letters, Section B: Nuclear, Elementary Particle and High-Energy Physics</i> , 2016, 762, 376-388.	3.0	30
184	Observation of inclined EeV air showers with the radio detector of the Pierre Auger Observatory. <i>Journal of Cosmology and Astroparticle Physics</i> , 2018, 2018, 026-026.	5.4	30
185	A SEARCH FOR POINT SOURCES OF EeV PHOTONS. <i>Astrophysical Journal</i> , 2014, 789, 160.	4.5	29
186	Particle identification in ALICE: a Bayesian approach. <i>European Physical Journal Plus</i> , 2016, 131, 1.	2.6	29
187	Centrality dependence of inclusive J/ψ production in p-Pb collisions at $s_{NN} = 5.02 \text{ TeV}$. <i>Journal of High Energy Physics</i> , 2015, 2015, 1.	4.7	28
188	Search for Very High-energy Gamma Rays from the Northern Fermi Bubble Region with HAWC. <i>Astrophysical Journal</i> , 2017, 842, 85.	4.5	28
189	Production of π^0 and η mesons up to high transverse momentum in pp collisions at 2.76 TeV. <i>European Physical Journal C</i> , 2017, 77, 339.	3.9	28
190	Constraints on jet quenching in p+Pb collisions at $s_{NN}=5.02 \text{ TeV}$ measured by the event-activity dependence of semi-inclusive hadron-jet distributions. <i>Physics Letters, Section B: Nuclear, Elementary Particle and High-Energy Physics</i> , 2018, 783, 95-113.	4.1	28
191	Production of π^0 and η mesons up to high transverse momentum in pp collisions at 2.76 TeV. <i>European Physical Journal C</i> , 2017, 77, 339.	3.9	27
192	A SEARCH FOR POINT SOURCES OF EeV NEUTRONS. <i>Astrophysical Journal</i> , 2012, 760, 148.	4.5	27
193	Interpretation of the depths of maximum of extensive air showers measured by the Pierre Auger Observatory. <i>Journal of Cosmology and Astroparticle Physics</i> , 2013, 2013, 026-026.	5.4	27
194	Event-shape engineering for inclusive spectra and elliptic flow in Pb-Pb collisions at $\sqrt{s_{NN}} = 2.76 \text{ TeV}$. <i>Physical Review C</i> , 2016, 93, 054902.	4.1	27
195	Multiplicity dependence of (anti)deuteron production in pp collisions at $\sqrt{s_{NN}} = 2.76 \text{ TeV}$. <i>Physics Letters, Section B: Nuclear, Elementary Particle and High-Energy Physics</i> , 2019, 790, 89-101.	4.1	27
196	Multiplicity dependence of (anti)deuteron production in pp collisions at $\sqrt{s_{NN}} = 2.76 \text{ TeV}$. <i>Physics Letters, Section B: Nuclear, Elementary Particle and High-Energy Physics</i> , 2019, 790, 89-101.	4.1	27
197	Measuring η' in p+Pb collisions at $\sqrt{s_{NN}} = 2.76 \text{ TeV}$. <i>Physics Letters, Section B: Nuclear, Elementary Particle and High-Energy Physics</i> , 2020, 800, 135043.	4.1	27
198	Interactions using Pb+Pb collisions at $\sqrt{s_{NN}} = 2.76 \text{ TeV}$. <i>Physics Letters, Section B: Nuclear, Elementary Particle and High-Energy Physics</i> , 2020, 800, 135043.	4.1	25

#	ARTICLE	IF	CITATIONS
199	Systematic studies of correlations between different order flow harmonics in Pb-Pb collisions at $\sqrt{s_{NN}} = 2.76 \text{ TeV}$. Physical Review C, 2018, 97, .	4.5	25
200	Observation of Anisotropy of TeV Cosmic Rays with Two Years of HAWC. Astrophysical Journal, 2018, 865, 57.	4.5	25
201	The effect of the geomagnetic field on cosmic ray energy estimates and large scale anisotropy searches on data from the Pierre Auger Observatory. Journal of Cosmology and Astroparticle Physics, 2011, 2011, 022-022.	5.4	24
202	The rapid atmospheric monitoring system of the Pierre Auger Observatory. Journal of Instrumentation, 2012, 7, P09001-P09001.	1.2	24
203	Results of a self-triggered prototype system for radio-detection of extensive air showers at the Pierre Auger Observatory. Journal of Instrumentation, 2012, 7, P11023-P11023.	1.2	24
204	Techniques for measuring aerosol attenuation using the Central Laser Facility at the Pierre Auger Observatory. Journal of Instrumentation, 2013, 8, P04009-P04009.	1.2	24
205	Milagro limits and HAWC sensitivity for the rate-density of evaporating Primordial Black Holes. Astroparticle Physics, 2015, 64, 4-12.	4.3	24
206	Measurement of the production of high-pT electrons from heavy-flavour hadron decays in Pb-Pb collisions at $\sqrt{s_{NN}} = 2.76 \text{ TeV}$. Physics Letters, Section B: Nuclear, Elementary Particle and High-Energy Physics, 2017, 771, 467-481.	4.1	24
207	Measurement of the production of high-pT electrons from heavy-flavour hadron decays in Pb-Pb collisions at $\sqrt{s_{NN}} = 5.02 \text{ TeV}$. Physics Letters, Section B: Nuclear, Elementary Particle and High-Energy Physics, 2018, 780, 7-20.	4.1	24
208	(Anti-)deuteron production in pp collisions at $\sqrt{s} = 13 \text{ TeV}$. European Physical Journal C, 2020, 80, 1.	3.9	24
209	Elliptic flow of muons from heavy-flavour hadron decays at forward rapidity in Pb-Pb collisions at $\sqrt{s_{NN}} = 2.76 \text{ TeV}$. Physics Letters, Section B: Nuclear, Elementary Particle and High-Energy Physics, 2016, 753, 41-56.	2.7	23
210	Azimuthal anisotropy of charged jet production in Pb-Pb collisions. Physics Letters, Section B: Nuclear, Elementary Particle and High-Energy Physics, 2016, 753, 511-525.	2.7	23
211	Measurement of azimuthal correlations of D mesons with charged particles in pp collisions at $\sqrt{s} = 7 \text{ TeV}$ and $\sqrt{s} = 5.02 \text{ TeV}$. European Physical Journal C, 2017, 77, 245.	3.9	23
212	Production of light-flavor hadrons in pp collisions at $\sqrt{s} \approx 13 \text{ TeV}$. European Physical Journal C, 2021, 81, 1.	3.9	23
213	Prompt D0, D+, and D*+ production in Pb-Pb collisions at $\sqrt{s_{NN}} = 5.02 \text{ TeV}$. Journal of High Energy Physics, 2022, 2022, 1.	4.7	23
214	Azimuthal asymmetry in the risetime of the surface detector signals of the Pierre Auger Observatory. Physical Review D, 2016, 93, .	4.7	21
215	A Targeted Search for Point Sources of EeV Photons with the Pierre Auger Observatory. Astrophysical Journal Letters, 2017, 837, L25.	8.3	21
216	Kaon femtoscopy in Pb-Pb collisions at $\sqrt{s_{NN}} = 2.76 \text{ TeV}$. Physical Review C, 2017, 96, .	2.9	21

#	ARTICLE	IF	CITATIONS
217	Calibration of the logarithmic-periodic dipole antenna (LPDA) radio stations at the Pierre Auger Observatory using an octocopter. <i>Journal of Instrumentation</i> , 2017, 12, T10005-T10005.	1.2	21
218	VERITAS and Fermi-LAT Observations of TeV Gamma-Ray Sources Discovered by HAWC in the 2HWC Catalog. <i>Astrophysical Journal</i> , 2018, 866, 24.	4.5	21
219	A Search for Photons with Energies Above 2×10^{17} eV Using Hybrid Data from the Low-Energy Extensions of the Pierre Auger Observatory. <i>Astrophysical Journal</i> , 2022, 933, 125.	4.5	21
220	Measurement of the cosmic ray spectrum above 4×10^{18} eV using inclined events detected with the Pierre Auger Observatory. <i>Journal of Cosmology and Astroparticle Physics</i> , 2015, 2015, 049-049.	5.4	20
221	Jet-like correlations with neutral pion triggers in pp and central Pb-Pb collisions at 2.76 TeV. <i>Physics Letters, Section B: Nuclear, Elementary Particle and High-Energy Physics</i> , 2016, 763, 238-250.	4.1	20
222	Nanosecond-level time synchronization of autonomous radio detector stations for extensive air showers. <i>Journal of Instrumentation</i> , 2016, 11, P01018-P01018.	1.2	20
223	Medium modification of the shape of small-radius jets in central Pb-Pb collisions at $\sqrt{s_{\text{NN}}} = 2.76$ TeV. <i>Journal of High Energy Physics</i> , 2018, 2018, 1.	4.7	20
224	meson in and Pb-Pb collisions at . <i>Physical Review C</i> , 2019, 99, .	2.9	20
225	Data-driven estimation of the invisible energy of cosmic ray showers with the Pierre Auger Observatory. <i>Physical Review D</i> , 2019, 100, .	4.7	20
226	Multi-Messenger Physics With the Pierre Auger Observatory. <i>Frontiers in Astronomy and Space Sciences</i> , 2019, 6, .	2.8	20
227	Suppression of resonance production in central Pb-Pb collisions at . <i>Physical Review C</i> , 2019, 99, .	2.9	20
228	Reconstruction of events recorded with the surface detector of the Pierre Auger Observatory. <i>Journal of Instrumentation</i> , 2020, 15, P10021-P10021.	1.2	20
229	Exploration of jet substructure using iterative declustering in pp and Pb-Pb collisions at LHC energies. <i>Physics Letters, Section B: Nuclear, Elementary Particle and High-Energy Physics</i> , 2020, 802, 125507.	4.1	20
230	Measurement of dijet in $\text{p} \bar{\text{p}}$ collisions at . <i>Physical Review C</i> , 2019, 99, .	4.1	19
231	Measurement of D s + production and nuclear modification factor in Pb-Pb collisions at $s_N = 2.76$ TeV. <i>Journal of High Energy Physics</i> , 2016, 2016, 1.	4.7	19
232	First HAWC observations of the Sun constrain steady TeV gamma-ray emission. <i>Physical Review D</i> , 2018, 98, .	4.7	19
233	Direct photon production at low transverse momentum in proton-proton collisions at $s=2.76$ and 8 TeV. <i>Physical Review C</i> , 2019, 99, .	2.9	19
234	Elliptic flow of electrons from heavy-flavour hadron decays at mid-rapidity in Pb-Pb collisions at $s_N = 2.76$ TeV. <i>Journal of High Energy Physics</i> , 2016, 2016, 1.	4.7	18

#	ARTICLE	IF	CITATIONS
235	Limits on point-like sources of ultra-high-energy neutrinos with the Pierre Auger Observatory. Journal of Cosmology and Astroparticle Physics, 2019, 2019, 004-004.	5.4	18
236	Energy dependence of $\tilde{\chi}(1020)$ production at mid-rapidity in pp collisions with ALICE at the LHC. Nuclear Physics A, 2019, 982, 180-182.	1.5	18
237	Azimuthal Anisotropy of Heavy-Flavor Decay Electrons in π^- -Pb Collisions at $\sqrt{s_{NN}} = 5.02$ TeV. Physical Review Letters, 2019, 122, 072301.	7.8	18
238	Measurement of prompt D0, D+, D*+, and $\psi(3770)$ production in p-Pb collisions at $\sqrt{s_{NN}} = 5.02$ TeV. Journal of High Energy Physics, 2019, 2019, 1.	4.7	18
239	Search for gamma-ray spectral lines from dark matter annihilation in dwarf galaxies with the High-Altitude Water Cherenkov observatory. Physical Review D, 2020, 101, .	4.7	18
240	Coherent $\psi(3770)$ photoproduction at midrapidity in ultra-peripheral Pb-Pb collisions at $\sqrt{s_{NN}} \approx 5.02$ TeV. European Physical Journal C, 2021, 81, 1.	3.9	18
241	Centrality dependence of $\tilde{\chi}(2S)$ suppression in p-Pb collisions at $\sqrt{s_{NN}} = 5.02$ TeV. Journal of High Energy Physics, 2016, 2016, 1.	4.7	17
242	The ALICE Transition Radiation Detector: Construction, operation, and performance. Nuclear Instruments and Methods in Physics Research, Section A: Accelerators, Spectrometers, Detectors and Associated Equipment, 2018, 881, 88-127.	1.6	17
243	Analysis of the apparent nuclear modification in peripheral Pb-Pb collisions at 5.02 TeV. Physics Letters, Section B: Nuclear, Elementary Particle and High-Energy Physics, 2019, 793, 420-432.	4.1	17
244	Measurement of beauty and charm production in pp collisions at $\sqrt{s} = 5.02$ TeV via non-prompt and prompt D mesons. Journal of High Energy Physics, 2021, 2021, 1.	4.7	17
245	The Pierre Auger Observatory scaler mode for the study of solar activity modulation of galactic cosmic rays. Journal of Instrumentation, 2011, 6, P01003-P01003.	1.2	16
246	The Lateral Trigger Probability function for the Ultra-High Energy Cosmic Ray showers detected by the Pierre Auger Observatory. Astroparticle Physics, 2011, 35, 266-276.	4.3	16
247	Muon counting using silicon photomultipliers in the AMIGA detector of the Pierre Auger observatory. Journal of Instrumentation, 2017, 12, P03002-P03002.	1.2	16
248	The HAWC Real-time Flare Monitor for Rapid Detection of Transient Events. Astrophysical Journal, 2017, 843, 116.	4.5	16
249	Data acquisition architecture and online processing system for the HAWC gamma-ray observatory. Nuclear Instruments and Methods in Physics Research, Section A: Accelerators, Spectrometers, Detectors and Associated Equipment, 2018, 888, 138-146.	1.6	16
250	Prompt and non-prompt $\psi(3770)$ production and nuclear modification at mid-rapidity in p-Pb collisions at $\sqrt{s_{NN}} = 5.02$ TeV. European Physical Journal C, 2018, 78, 1.	3.9	16
251	Hadronic resonances, strange and multi-strange particle production in Xe-Xe and Pb-Pb collisions with ALICE at the LHC. Nuclear Physics A, 2019, 982, 823-826.	1.5	16
252	Testing the system size dependence of hydrodynamical expansion and thermal particle production with π^+ , K, p, and \bar{p} in Xe-Xe and Pb-Pb collisions with ALICE. Nuclear Physics A, 2019, 982, 427-430.	1.5	16

#	ARTICLE	IF	CITATIONS
253	Event-Shape Engineering for the D-meson elliptic flow in mid-central Pb-Pb collisions at $\sqrt{s_{\text{NN}}} = 5.02 \text{ TeV}$. Journal of High Energy Physics, 2019, 2019, 1.	4.7	16
254	Constraining the local burst rate density of primordial black holes with HAWC. Journal of Cosmology and Astroparticle Physics, 2020, 2020, 026-026.	5.4	16
255	Deep-learning based reconstruction of the shower maximum X_{max} using the water-Cherenkov detectors of the Pierre Auger Observatory. Journal of Instrumentation, 2021, 16, P07019.	1.2	16
256	Search for ultrarelativistic magnetic monopoles with the Pierre Auger observatory. Physical Review D, 2016, 94, .	4.7	15
257	Relative particle yield fluctuations in Pb-Pb collisions at $\sqrt{s_{\text{NN}}} = 2.76 \text{ TeV}$. European Physical Journal C, 2019, 79, 1.	3.9	15
258	Higher harmonic non-linear flow modes of charged hadrons in Pb-Pb collisions at $\sqrt{s_{\text{NN}}} = 5.02 \text{ TeV}$. Journal of High Energy Physics, 2020, 2020, 1.	4.7	15
259	Constraining the Chiral Magnetic Effect with charge-dependent azimuthal correlations in Pb-Pb collisions at $\sqrt{s_{\text{NN}}} = 2.76$ and 5.02 TeV . Journal of High Energy Physics, 2020, 2020, 1.	4.7	15
260	A TARGETED SEARCH FOR POINT SOURCES OF EeV NEUTRONS. Astrophysical Journal Letters, 2014, 789, L34.	8.3	14
261	Multi-resolution anisotropy studies of ultrahigh-energy cosmic rays detected at the Pierre Auger Observatory. Journal of Cosmology and Astroparticle Physics, 2017, 2017, 026-026. First measurement of $\langle \sin(\theta) \rangle$ at $\sqrt{s_{\text{NN}}} = 5.02 \text{ TeV}$. 	5.4	14
262	$\langle \cos(2\phi) \rangle$ at $\sqrt{s_{\text{NN}}} = 5.02 \text{ TeV}$. 	5.4	14
263	Real-time data processing in the ALICE High Level Trigger at the LHC. Computer Physics Communications, 2019, 242, 25-48.	7.5	14
264	Measurement of dielectron production in central Pb-Pb collisions at $\sqrt{s_{\text{NN}}} = 5.02 \text{ TeV}$. Physical Review C, 2019, 99, .	4.1	14
265	J/ψ elliptic and triangular flow in Pb-Pb collisions at $\sqrt{s_{\text{NN}}} = 5.02 \text{ TeV}$. Journal of High Energy Physics, 2020, 2020, 1.	4.7	14
266	Measurement of strange baryon-antibaryon interactions with femtoscopic correlations. Physics Letters, Section B: Nuclear, Elementary Particle and High-Energy Physics, 2020, 802, 135223.	4.1	14
267	Spectrum and Morphology of the Very-high-energy Source HAWC J2019+368. Astrophysical Journal, 2021, 911, 143.	4.5	14
268	Inclusive J/ψ production at mid-rapidity in pp collisions at $\sqrt{s} = 5.02 \text{ TeV}$. Journal of High Energy Physics, 2019, 2019, 1.	4.7	14
269	W and Z boson production in p-Pb collisions at $s_{\text{NN}} = 5.02 \text{ TeV}$. Journal of High Energy Physics, 2017, 2017, 1.	4.7	13
270	Anomalous Evolution of the Near-Side Jet Peak Shape in Pb-Pb Collisions at $\sqrt{s_{\text{NN}}} = 5.02 \text{ TeV}$. 	4.7	13

#	ARTICLE	IF	CITATIONS
271	Searches for transverse momentum dependent flow vector fluctuations in Pb-Pb and p-Pb collisions at the LHC. <i>Journal of High Energy Physics</i> , 2017, 2017, 1.	4.7	13
272	Neutral pion and $\bar{\ell}$ meson production at midrapidity in Pb-Pb collisions at $s_{\text{NN}}=2.76 \text{ TeV}$. <i>Physical Review C</i> , 2018, 98, .	2.9	13
273	Measurement of the inclusive J/ψ polarization at forward rapidity in pp collisions at $\sqrt{s} = 8 \text{ TeV}$. <i>European Physical Journal C</i> , 2018, 78, 1.	3.9	13
274	Studies of J/ψ production at forward rapidity in Pb-Pb collisions at $\sqrt{s_{\text{NN}}} = 5.02 \text{ TeV}$. <i>Journal of High Energy Physics</i> , 2020, 2020, 1.	4.7	13
275	A Survey of Active Galaxies at TeV Photon Energies with the HAWC Gamma-Ray Observatory. <i>Astrophysical Journal</i> , 2021, 907, 67.	4.5	13
276	Design, upgrade and characterization of the silicon photomultiplier front-end for the AMIGA detector at the Pierre Auger Observatory. <i>Journal of Instrumentation</i> , 2021, 16, P01026-P01026.	1.2	13
277	A Search for Ultra-high-energy Neutrinos from TXS 0506+056 Using the Pierre Auger Observatory. <i>Astrophysical Journal</i> , 2020, 902, 105.	4.5	13
278	Search for patterns by combining cosmic-ray energy and arrival directions at the Pierre Auger Observatory. <i>European Physical Journal C</i> , 2015, 75, 269.	3.9	12
279	Search for Very-high-energy Emission from Gamma-Ray Bursts Using the First 18 Months of Data from the HAWC Gamma-Ray Observatory. <i>Astrophysical Journal</i> , 2017, 843, 88.	4.5	12
280	Azimuthally Differential Pion Femtoscopy in Pb-Pb Collisions at $s_{\text{NN}}=2.76 \text{ TeV}$. <i>Physical Review Letters</i> , 2017, 118, 222301.	7.8	12
281	J/ψ production as a function of charged-particle pseudorapidity density in p-Pb collisions at $\sqrt{s_{\text{NN}}} = 5.02 \text{ TeV}$. <i>Nuclear Physics A</i> , 2019, 982, 467-470.	4.1	12
282	Charged-particle pseudorapidity density at mid-rapidity in p-Pb collisions at $\sqrt{s_{\text{NN}}} = 8.16 \text{ TeV}$. <i>European Physical Journal C</i> , 2019, 79, 1.	3.9	12
283	Multiplicity dependence of strangeness and hadronic resonance production in pp and p-Pb collisions with ALICE at the LHC. <i>Nuclear Physics A</i> , 2019, 982, 467-470.	1.5	12
284	Measuring $\langle \text{pT}^2 \rangle$ in p-Pb collisions at $\sqrt{s_{\text{NN}}} = 5.02 \text{ TeV}$. <i>Nuclear Physics A</i> , 2019, 982, 467-470.	4.1	12
285	Study of J/ψ azimuthal anisotropy at forward rapidity in Pb-Pb collisions at $\sqrt{s_{\text{NN}}} = 5.02 \text{ TeV}$. <i>Journal of High Energy Physics</i> , 2019, 2019, 1.	4.7	12
286	Production of pions, kaons, (anti-)protons and ϕ mesons in Xe-Xe collisions at $\sqrt{s_{\text{NN}}} = 5.44 \text{ TeV}$. <i>European Physical Journal C</i> , 2021, 81, 1.	3.9	12
287	Pseudorapidity distributions of charged particles as a function of mid- and forward rapidity multiplicities in pp collisions at $\sqrt{s} = 5.02, 7$ and 13 TeV . <i>European Physical Journal C</i> , 2021, 81, 1.	3.9	12
288	Cosmic ray spectrum of protons plus helium nuclei between 6 and 158 TeV from HAWC data. <i>Physical Review D</i> , 2022, 105, .	4.7	12

#	ARTICLE	IF	CITATIONS
289	UHE neutrino damping in a thermal gas of relic neutrinos. <i>Astroparticle Physics</i> , 2006, 25, 47-56.	4.3	11
290	VAMOS: A pathfinder for the HAWC gamma-ray observatory. <i>Astroparticle Physics</i> , 2015, 62, 125-133.	4.3	11
291	Search for dark matter gamma-ray emission from the Andromeda Galaxy with the High-Altitude Water Cherenkov Observatory. <i>Journal of Cosmology and Astroparticle Physics</i> , 2018, 2018, 043-043.	5.4	11
292	Combining Cherenkov and scintillation detector observations with simulations to deduce the nature of high-energy radiation excesses during thunderstorms. <i>Physical Review D</i> , 2019, 100, .	4.7	11
293	Measurement of the production of charm jets tagged with D0 mesons in pp collisions at $\sqrt{s} = 7 \text{ TeV}$. <i>Journal of High Energy Physics</i> , 2019, 2019, 1.	4.7	11
294	Dielectron and heavy-quark production in inelastic and high-multiplicity proton-proton collisions at $\sqrt{s} = 7 \text{ TeV}$. <i>Physics Letters, Section B: Nuclear, Elementary Particle and High-Energy Physics</i> , 2019, 788, 505-518.		
295	Azimuthal correlations of prompt D mesons with charged particles in pp and p-Pb collisions at $\sqrt{s_{\text{NN}}} = 5.02 \text{ TeV}$. <i>European Physical Journal C</i> , 2020, 80, 1.	3.9	11
296	Coherent photoproduction of Ω^0 vector mesons in ultra-peripheral Pb-Pb collisions at $\sqrt{s_{\text{NN}}} = 5.02 \text{ TeV}$. <i>Journal of High Energy Physics</i> , 2020, 2020, 1.	4.7	11
297	Extraction of the muon signals recorded with the surface detector of the Pierre Auger Observatory using recurrent neural networks. <i>Journal of Instrumentation</i> , 2021, 16, P07016.	1.2	11
298	Underlying event properties in pp collisions at $\sqrt{s} = 13 \text{ TeV}$. <i>Journal of High Energy Physics</i> , 2020, 2020, 1.	4.7	11
299	Measurement of the production cross section of prompt Ξ_c^0 baryons at midrapidity in pp collisions at $\sqrt{s} = 5.02 \text{ TeV}$. <i>Journal of High Energy Physics</i> , 2021, 2021, 1.	4.7	11
300	Measurement of D-meson production versus multiplicity in p-Pb collisions at $\sqrt{s_{\text{NN}}} = 5.02 \text{ TeV}$. <i>Journal of High Energy Physics</i> , 2016, 2016, 1.	4.7	10
301	Evolution of the longitudinal and azimuthal structure of the near-side jet peak in Pb-Pb collisions at $\sqrt{s_{\text{NN}}} = 5.02 \text{ TeV}$. <i>Physical Review C</i> , 2017, 96, 024906.		
302	Inclusive J/ψ production in Xe-Xe collisions at $\sqrt{s_{\text{NN}}} = 5.44 \text{ TeV}$. <i>Physical Review C</i> , 2018, 98, 054906.		
303	Measurement of the average shape of longitudinal profiles of cosmic-ray air showers at the Pierre Auger Observatory. <i>Journal of Cosmology and Astroparticle Physics</i> , 2019, 2019, 018-018.	5.4	10
304	Two-particle differential transverse momentum and number density correlations in p_T collisions at $\sqrt{s} = 5.02 \text{ TeV}$ and Pb-Pb collisions at $\sqrt{s} = 2.76 \text{ TeV}$ at the CERN Large Hadron Collider. <i>Physical Review C</i> , 2019, 100, .	2.9	10
305	Search for magnetically-induced signatures in the arrival directions of ultra-high-energy cosmic rays measured at the Pierre Auger Observatory. <i>Journal of Cosmology and Astroparticle Physics</i> , 2020, 2020, 017-017.	5.4	10
306	Measurement of $\Lambda(1520)$ production in pp collisions at $\sqrt{s} = 7 \text{ TeV}$ and p-Pb collisions at $\sqrt{s_{\text{NN}}} = 5.02 \text{ TeV}$. <i>European Physical Journal C</i> , 2020, 80, 1.	3.9	10

#	ARTICLE	IF	CITATIONS
307	Anisotropy and chemical composition of ultra-high energy cosmic rays using arrival directions measured by the Pierre Auger Observatory. <i>Journal of Cosmology and Astroparticle Physics</i> , 2011, 2011, 022-022.	5.4	9
308	Measurement of electrons from beauty-hadron decays in p-Pb collisions at $s = 5.02 \text{ TeV}$ and Pb-Pb collisions at $s = 2.76 \text{ TeV}$. <i>Journal of High Energy Physics</i> , 2017, 2017, 1.	4.7	9
309	Constraining the ratio in TeV cosmic rays with observations of the Moon shadow by HAWC. <i>Physical Review D</i> , 2018, 97,	4.7	9
310	Searching for dark matter sub-structure with HAWC. <i>Journal of Cosmology and Astroparticle Physics</i> , 2019, 2019, 022-022.	5.4	9
311	Event-shape and multiplicity dependence of freeze-out radii in pp collisions at $\sqrt{s} = 7 \text{ TeV}$. <i>Journal of High Energy Physics</i> , 2019, 2019, 1.	4.7	9
312	Event-shape- and multiplicity-dependent identified particle production in pp collisions at 13 TeV with ALICE at the LHC. <i>Nuclear Physics A</i> , 2019, 982, 507-510.	1.5	9
313	Charged jet cross section and fragmentation in proton-proton collisions at $\sqrt{s} = 13 \text{ TeV}$. <i>Physical Review D</i> , 2019, 99,	4.7	9
314	A 3-year Sample of Almost 1,600 Elves Recorded Above South America by the Pierre Auger Cosmic-Ray Observatory. <i>Earth and Space Science</i> , 2020, 7, e2019EA000582.	2.6	9
315	Probing the Sea of Cosmic Rays by Measuring Gamma-Ray Emission from Passive Giant Molecular Clouds with HAWC. <i>Astrophysical Journal</i> , 2021, 914, 106.	4.5	9
316	Multimessenger Gamma-Ray and Neutrino Coincidence Alerts Using HAWC and IceCube Subthreshold Data. <i>Astrophysical Journal</i> , 2021, 906, 63.	4.5	9
317	Production of light (anti)nuclei in pp collisions at $\sqrt{s} = 13 \text{ TeV}$. <i>Journal of High Energy Physics</i> , 2022, 2022, 1.	4.7	9
318	Publisher's Note: Search for ultrahigh energy neutrinos in highly inclined events at the Pierre Auger Observatory [Phys. Rev. D84, 122005 (2011)]. <i>Physical Review D</i> , 2012, 85, .	4.7	8
319	Identifying clouds over the Pierre Auger Observatory using infrared satellite data. <i>Astroparticle Physics</i> , 2013, 50-52, 92-101.	4.3	8
320	Impact of atmospheric effects on the energy reconstruction of air showers observed by the surface detectors of the Pierre Auger Observatory. <i>Journal of Instrumentation</i> , 2017, 12, P02006-P02006.	1.2	8
321	Flow Dominance and Factorization of Transverse Momentum Correlations in Pb-Pb Collisions at the LHC. <i>Physical Review Letters</i> , 2017, 118, 162302.	7.8	8
322	Inclusive J/ψ production at forward and backward rapidity in p-Pb collisions at $\sqrt{s} = 8.16 \text{ TeV}$. <i>Journal of High Energy Physics</i> , 2018, 2018, 1.	4.7	8
323	Calibration of the photon spectrometer PHOS of the ALICE experiment. <i>Journal of Instrumentation</i> , 2019, 14, P05025-P05025.	1.2	8
324	Elliptic flow of identified hadrons in small collisional systems measured with ALICE. <i>Nuclear Physics A</i> , 2019, 982, 451-454.	1.5	8

#	ARTICLE		IF	CITATIONS
325	Measurement of charged jet cross section in Pb-Pb collisions at $s_{\text{NN}}=5.02 \text{ TeV}$. <i>Physical Review D</i> , 2019, 100.,	$\text{display}=\text{"block"}$ $\text{display}=\text{"block"}$	4.7	8
326	Measurement of the inclusive isolated photon production cross section in pp collisions at $\sqrt{s}=7 \text{ TeV}$. <i>European Physical Journal C</i> , 2019, 79, 1.	$\text{display}=\text{"block"}$	3.9	8
327	Long-term Spectra of the Blazars Mrk 421 and Mrk 501 at TeV Energies Seen by HAWC. <i>Astrophysical Journal</i> , 2022, 929, 125.		4.5	8
328	N-string amplitude as a trace of half-string matrices. <i>Physical Review D</i> , 1989, 40, 2620-2625.		4.7	7
329	Calibration and monitoring of water Cherenkov detectors with stopping and crossing muons. <i>Nuclear Instruments and Methods in Physics Research, Section A: Accelerators, Spectrometers, Detectors and Associated Equipment</i> , 1999, 420, 39-47.		1.6	7
330	Spectral calibration of the fluorescence telescopes of the Pierre Auger Observatory. <i>Astroparticle Physics</i> , 2017, 95, 44-56.		4.3	7
331	Measurements of low-pT electrons from semileptonic heavy-flavour hadron decays at mid-rapidity in pp and Pb-Pb collisions at $\sqrt{s_{\text{NN}}}=2.76 \text{ TeV}$. <i>Journal of High Energy Physics</i> , 2018, 2018, 1.		4.7	7
332	Measurement of Z0-boson production at large rapidities in Pb-Pb collisions at $s_{\text{NN}}=5.02 \text{ TeV}$. <i>Physics Letters, Section B: Nuclear, Elementary Particle and High-Energy Physics</i> , 2018, 780, 372-383.		4.1	7
333	Measurement of jet radial profiles in Pb-Pb collisions at $\sqrt{s_{\text{NN}}}=2.76 \text{ TeV}$. <i>One-dimensional charged kaon femtoscopy in Pb-Pb collisions at $\sqrt{s_{\text{NN}}}=2.76 \text{ TeV}$</i> .	$\text{display}=\text{"block"}$ $\text{display}=\text{"block"}$	4.1	7
334	ALICE measurements of flow coefficients and their correlations in small (pp and p-Pb) and large (Xe-Xe and Pb-Pb) collision systems. <i>Nuclear Physics A</i> , 2019, 982, 487-490.	$\text{display}=\text{"block"}$	2.9	7
335	Higher moment fluctuations of identified particle distributions from ALICE. <i>Nuclear Physics A</i> , 2019, 982, 851-854.		1.5	7
336	MAGIC and <i>Fermi</i> -LAT gamma-ray results on unassociated HAWC sources. <i>Monthly Notices of the Royal Astronomical Society</i> , 2019, 485, 356-366.		4.4	7
337	Fair Weather Neutron Bursts From Photonuclear Reactions by Extensive Air Shower Core Interactions in the Ground and Implications for Terrestrial Gamma-ray Flash Signatures. <i>Geophysical Research Letters</i> , 2021, 48, e2020GL090033.		4.0	7
338	Production of light (anti)nuclei in pp collisions at $\sqrt{s}=5.02 \text{ TeV}$. <i>European Physical Journal C</i> , 2022, 82, 1.		3.9	7
340	New expressions for string loop amplitudes leading to an ultrasimple conception of string dynamics. <i>Physical Review D</i> , 1991, 44, 1786-1800.		4.7	6
341	Degeneracy of Resonances: Branch Point and Branch Cuts in Parameter Space. <i>International Journal of Theoretical Physics</i> , 2007, 46, 1666-1701.		1.2	6
342	A search for anisotropy in the arrival directions of ultra high energy cosmic rays recorded at the Pierre Auger Observatory. <i>Journal of Cosmology and Astroparticle Physics</i> , 2012, 2012, 040-040.		5.4	6

#	ARTICLE	IF	CITATIONS
343	Origin of atmospheric aerosols at the Pierre Auger Observatory using studies of air mass trajectories in South America. <i>Atmospheric Research</i> , 2014, 149, 120-135.	4.1	6
344	Production of muons from heavy-flavour hadron decays in $\bar{p}p$ collisions at $\sqrt{s} = 5.02 \text{ TeV}$. <i>Nuclear Physics Letters, Section B: Nuclear, Elementary Particle and High-Energy Physics</i> , 2017, 770, 459-472.	6	
345	Addendum to: Centrality dependence of high-pT D-meson suppression in Pb-Pb collisions at $\sqrt{s_NN} = 2.76 \text{ TeV}$. <i>Journal of High Energy Physics</i> , 2017, 2017, 1.	4.7	6
346	Dielectron production in proton-proton collisions at $\sqrt{s} = 7 \text{ TeV}$. <i>Journal of High Energy Physics</i> , 2018, 2018, 1.	4.7	6
347	Spin alignment measurements using vector mesons with ALICE detector at the LHC. <i>Nuclear Physics A</i> , 2019, 982, 515-518.	1.5	6
348	Measurement of nuclear effects on $\bar{\chi}(2S)$ production in p-Pb collisions at $\sqrt{s_{NN}} = 8.16 \text{ TeV}$. <i>Journal of High Energy Physics</i> , 2020, 2020, 1.	4.7	6
349	Measurement of inclusive charged-particle b-jet production in pp and p-Pb collisions at $\sqrt{s_{NN}} = 5.02 \text{ TeV}$. <i>Journal of High Energy Physics</i> , 2022, 2022, 1.	4.7	6
350	HAWC Study of the Ultra-high-energy Spectrum of MGRO J1908+06. <i>Astrophysical Journal</i> , 2022, 928, 116.	4.5	6
351	Inclusive $\psi(2S)$ production at midrapidity in pp collisions at $\sqrt{s} = 13 \text{ TeV}$. <i>European Physical Journal C</i> , 2021, 81, 1.	3.9	6
352	Investigating charm production and fragmentation via azimuthal correlations of prompt D mesons with charged particles in pp collisions at $\sqrt{s} = 13 \text{ TeV}$. <i>European Physical Journal C</i> , 2022, 82, 1.	3.9	6
353	The observation of a muon deficit in simulations from data of the Pierre Auger Observatory. <i>Journal of Physics: Conference Series</i> , 2013, 409, 012107.	0.4	5
354	Exploring the Phase Space of Jet Splittings at ALICE using Grooming and Recursive Techniques. <i>Nuclear Physics A</i> , 2019, 982, 587-590.	1.5	5
355	Balance functions of (un)identified hadrons in $\bar{p}p$, $\bar{p}p$, and pp collisions at the LHC. <i>Nuclear Physics A</i> , 2019, 982, 315-318.	1.5	5
356	Energy and system dependence of nuclear modification factors of inclusive charged particles and identified light hadrons measured in $\bar{p}p$, $Xe\bar{p}$ and $\bar{p}p$ collisions with ALICE. <i>Nuclear Physics A</i> , 2019, 982, 567-570.	1.5	5
357	Addressing the hypertriton lifetime puzzle with ALICE at the LHC. <i>Nuclear Physics A</i> , 2019, 982, 815-818.	1.5	5
358	Jet fragmentation transverse momentum measurements from di-hadron correlations in pp and $\sqrt{s_{NN}} = 5.02 \text{ TeV}$ $\bar{p}p$ collisions. <i>Journal of High Energy Physics</i> , 2019, 2019, 1.	4.7	5
359	Studies on the response of a water-Cherenkov detector of the Pierre Auger Observatory to atmospheric muons using an RPC hodoscope. <i>Journal of Instrumentation</i> , 2020, 15, P09002-P09002.	1.2	5
360	Calibration of the underground muon detector of the Pierre Auger Observatory. <i>Journal of Instrumentation</i> , 2021, 16, P04003.	1.2	5

#	ARTICLE	IF	CITATIONS
361	Long- and short-range correlations and their event-scale dependence in high-multiplicity pp collisions at $\sqrt{s} = 13$ TeV. <i>Journal of High Energy Physics</i> , 2021, 2021, 1.	4.7	5
362	Energy dependence of ϕ meson production at forward rapidity in pp collisions at the LHC. <i>European Physical Journal C</i> , 2021, 81, 1.	3.9	5
363	HAWC and Fermi-LAT Detection of Extended Emission from the Unidentified Source 2HWC J2006+341. <i>Astrophysical Journal Letters</i> , 2020, 903, L14.	8.3	5
364	Anisotropic flow of identified hadrons in Xe-Xe collisions at $\sqrt{s_{\text{NN}}} = 5.44$ TeV. <i>Journal of High Energy Physics</i> , 2021, 2021, 1.	4.7	5
365	Testing effects of Lorentz invariance violation in the propagation of astroparticles with the Pierre Auger Observatory. <i>Journal of Cosmology and Astroparticle Physics</i> , 2022, 2022, 023. Longitudinal asymmetry and its effect on pseudorapidity distributions in Pb-Pb collisions at $\sqrt{s_{\text{NN}}} = 2.76$ TeV. <i>Nuclear Physics Letters, Section B: Nuclear, Elementary Particle and High-Energy Physics</i> , 2018, 781, 20-32.	5.4	5
366	Light (anti-)nuclei production and elliptic flow at the LHC with ALICE. <i>Nuclear Physics A</i> , 2019, 982, 447-450.	4.1	4
367	ALICE results on system-size dependence of charged-particle multiplicity density in p-Pb, Pb-Pb and Xe-Xe collisions. <i>Nuclear Physics A</i> , 2019, 982, 279-282.	1.5	4
368	Measurements of the chiral magnetic effect in Pb-Pb collisions with ALICE. <i>Nuclear Physics A</i> , 2019, 982, 543-546.	1.5	4
369	Investigating correlated fluctuations of conserved charges with net- $\hat{\ell}$ fluctuations in Pb-Pb collisions at ALICE. <i>Nuclear Physics A</i> , 2019, 982, 299-302.	1.5	4
370	Production of muons from heavy-flavour hadron decays in pp collisions at $\sqrt{s} = 5.02$ TeV. <i>Journal of High Energy Physics</i> , 2019, 2019, 1.	4.7	4
371	J/ψ production as a function of charged-particle multiplicity in p-Pb collisions at $\sqrt{s_{\text{NN}}} = 8.16$ TeV. <i>Journal of High Energy Physics</i> , 2020, 2020, 1.	4.7	4
372	Measurement of electrons from heavy-flavour hadron decays as a function of multiplicity in p-Pb collisions at $\sqrt{s_{\text{NN}}} = 5.02$ TeV. <i>Journal of High Energy Physics</i> , 2020, 2020, 1.	4.7	4
373	Non-linear flow modes of identified particles in Pb-Pb collisions at $\sqrt{s_{\text{NN}}} = 5.02$ TeV. <i>Journal of High Energy Physics</i> , 2020, 2020, 1.	4.7	4
374	Centrality dependence of J/ψ and Υ(2S) production and nuclear modification in p-Pb collisions at $\sqrt{s_{\text{NN}}} = 8.16$ TeV. <i>Journal of High Energy Physics</i> , 2021, 2021, 1.	4.7	4
375	Production of omega mesons in pp collisions at $\sqrt{s} = 7$ TeV. <i>European Physical Journal C</i> , 2020, 80, 1.	3.9	4
376	Constraining the mSUGRA (minimal supergravity) parameter space using the entropy of dark matter halos. <i>Journal of Cosmology and Astroparticle Physics</i> , 2008, 2008, 003.	5.4	3
377	The Pierre Auger Observatory offline software. <i>Journal of Physics: Conference Series</i> , 2008, 119, 032002.	0.4	3

#	ARTICLE	IF	CITATIONS
379	ϕ meson production at forward rapidity in Pb-Pb collisions at $\sqrt{s_{\text{NN}}} = 2.76 \text{ TeV}$. European Physical Journal C, 2018, 78, 1.	3.9	3
380	HAWC Search for High-mass Microquasars. Astrophysical Journal Letters, 2021, 912, L4.	8.3	3
381	Design and implementation of the AMIGA embedded system for data acquisition. Journal of Instrumentation, 2021, 16, T07008.	1.2	3
382	Gamma/hadron separation with the HAWC observatory. Nuclear Instruments and Methods in Physics Research, Section A: Accelerators, Spectrometers, Detectors and Associated Equipment, 2022, 1039, 166984.	1.6	3
383	The Pierre Auger Observatory status and latest results. EPJ Web of Conferences, 2017, 136, 02017.	0.3	2
384	Quarkonium measurements in nucleus-nucleus collisions with ALICE. Nuclear Physics A, 2019, 982, 703-706.	1.5	2
385	Measurements of heavy-flavour correlations and jets with ALICE at the LHC. Nuclear Physics A, 2019, 982, 579-582.	1.5	2
386	Upgrade of the ALICE central barrel tracking detectors: ITS and TPC. Nuclear Physics A, 2019, 982, 943-946.	1.5	2
387	Dielectron measurements in pp and Pb-Pb collisions with ALICE at the LHC. Nuclear Physics A, 2019, 982, 779-782.	1.5	2
388	Measurements of anisotropic flow and flow fluctuations in Xe-Xe and Pb-Pb collisions with ALICE. Nuclear Physics A, 2019, 982, 367-370.	1.5	2
389	HAWC as a Ground-Based Space-Weather Observatory. Solar Physics, 2021, 296, 1.	2.5	2
390	The High Altitude Water Čerenkov (HAWC) TeV Gamma Ray Observatory. Thirty Years of Astronomical Discovery With UKIRT, 2013, , 439-446.	0.3	2
391	The potential of the HAWC Observatory to observe violations of Lorentz Invariance. , 2016, , .	2	
392	Interplanetary Magnetic Flux Rope Observed at Ground Level by HAWC. Astrophysical Journal, 2020, 905, 73.	4.5	2
393	Charged-particle multiplicity fluctuations in Pb-Pb collisions at $\sqrt{s_{\text{NN}}} = 2.76 \text{ TeV}$. European Physical Journal C, 2021, 81, 1.	3.9	2
394	Characterization of the background for a neutrino search with the HAWC observatory. Astroparticle Physics, 2022, 137, 102670.	4.3	2
395	FUNDAMENTALLY NEW PHYSICS AT THE TEVATRON COLLIDER?. International Journal of Modern Physics A, 1989, 04, 5003-5009.	1.5	1
396	Entropy considerations in constraining the mSUGRA parameter space. AIP Conference Proceedings, 2006, , .	0.4	1

#	ARTICLE	IF	CITATIONS
397	Azimuthally-differential pion femtoscopy relative to the third harmonic event plane in Pb-Pb collisions at sNN=2.76TeV. Physics Letters, Section B: Nuclear, Elementary Particle and High-Energy Physics, 2018, 785, 320-331.	4.1	1
398	f0(980) resonance production in pp collisions with the ALICE detector at the LHC. Nuclear Physics A, 2019, 982, 201-203.	1.5	1
399	Heavy-flavour hadron decay leptons in Pb-Pb and Xe-Xe collisions at the LHC with ALICE. Nuclear Physics A, 2019, 982, 651-654.	1.5	1
400	Muon physics at forward rapidity with the ALICE detector upgrade. Nuclear Physics A, 2019, 982, 947-950.	1.5	1
401	Quarkonium production in p-Pb collisions with ALICE. Nuclear Physics A, 2019, 982, 739-742.	1.5	1
402	Constraining production models with light (anti-)nuclei measurements in small systems with ALICE at the LHC. Nuclear Physics A, 2019, 982, 895-898.	1.5	1
403	ALICE Collaboration. Nuclear Physics A, 2019, 982, 975-984.	1.5	1
404	Constraints on the Emission of Gamma-Rays from M31 with HAWC. Astrophysical Journal, 2020, 893, 16.	4.5	1
405	Jet fragmentation transverse momentum distributions in pp and p-Pb collisions at $\sqrt{s} = 5.02 \text{ TeV}$. Journal of High Energy Physics, 2021, 2021, 1.	4.7	1
406	K_S^0 - and (anti-)Lambda-hadron correlations in pp collisions at $\sqrt{s} = 13 \text{ TeV}$. European Physical Journal C, 2021, 81, 1.	3.9	1
407	First measurements of N-subjettiness in central Pb-Pb collisions at $\sqrt{s_{\text{NN}}} = 2.76 \text{ TeV}$. Journal of High Energy Physics, 2021, 2021, 1.	4.7	1
408	Monitoring at TeV Energies with M@TE. , 2017, , .		1
409	Axial couplings in the world line formalism. , 1997, , .		0
410	Recent results on the operation of a Cherenkov detector prototype for the Pierre Auger observatory. , 1999, , .		0
411	Simulations of the surface detector of the Pierre Auger Observatory "Calibration and Monitoring". , 1999, , .		0
412	Stability and calibration of a water Čerenkov detector prototype. Nuclear Physics, Section B, Proceedings Supplements, 1999, 75, 389-391.	0.4	0
413	Ultra High Energy Neutrinos and their Detection in the Pierre Auger Observatory. AIP Conference Proceedings, 2002, , .	0.4	0
414	Near-horizontal Air Showers. AIP Conference Proceedings, 2003, , .	0.4	0

#	ARTICLE	IF	CITATIONS
415	The offline software framework of the pierre auger observatory., 0, , .	0	
416	The Offline Software Framework of the Pierre Auger Observatory. , 0, , .	0	
417	Unfolding a degeneracy point of two unbound states: crossings and anticrossings of energies and widths. , 0, , .	0	
418	The Pierre Auger Observatoryâ€”Status and first results. AIP Conference Proceedings, 2006, , .	0.4	0
419	Thermal effects on the absorption of ultra-high energy neutrinos by the cosmic neutrino background. Journal of Physics: Conference Series, 2006, 39, 422-425.	0.4	0
420	Constraining the mSUGRA parameter space through entropy and abundance criteria. AIP Conference Proceedings, 2007, , .	0.4	0
421	A study of the arrival direction using Offline. , 2009, , .	0	
422	The derivation of constraints on the msugra parameter space from the entropy of dark matter halos. , 2009, , .	0	
423	Signal fluctuations and multi-layer shower fronts. , 2009, , .	0	
424	The Pierre Auger Observatory: status, results and outlook. Nuclear Physics, Section B, Proceedings Supplements, 2009, 188, 233-238.	0.4	0
425	Search for UHE neutrinos in coincidence with LIGO GW150914 event with the Pierre Auger Observatory. Proceedings of the International Astronomical Union, 2016, 12, 295-298.	0.0	0
426	The Pierre Auger Observatory Upgrade. EPJ Web of Conferences, 2017, 136, 02003.	0.3	0
427	Exploiting the radio signal from air showers: the AERA progress. EPJ Web of Conferences, 2017, 136, 02013.	0.3	0
428	Astrophysical interpretation of Pierre Auger Observatory measurements of the UHECR energy spectrum and mass composition. EPJ Web of Conferences, 2017, 136, 02002.	0.3	0
429	Non-strange and strange D-meson and charm-baryon production in heavy-ion collisions measured with ALICE at the LHC. Nuclear Physics A, 2019, 982, 667-670.	1.5	0
430	The evolution of the near-side peak in two-particle number and transverse momentum correlations in Pbâ€“Pb collisions from ALICE. Nuclear Physics A, 2019, 982, 363-366.	1.5	0
431	Non-linear flow modes of identified particles in Pbâ€“Pb collisions at sNN=5.02TeV with the ALICE detector. Nuclear Physics A, 2019, 982, 383-386.	1.5	0
432	Electroweak boson measurements in p-Pb and Pb-Pb collisions at sNN=5.02TeV with ALICE at the LHC. Nuclear Physics A, 2019, 982, 783-786.	1.5	0

#	ARTICLE	IF	CITATIONS
433	Pion-kaon femtoscopy in Pb-Pb collisions at sNN=2.76TeV measured with ALICE. Nuclear Physics A, 2019, 982, 351-354.	1.5	0
434	Direct photon elliptic flow in Pb-Pb collisions at $\sqrt{s_{NN}} = 2.76 \text{ TeV}$. Nuclear Physics A, 2019, 982, 195-197.	1.5	0
435	Open heavy-flavour production and elliptic flow in p-Pb collisions at the LHC with ALICE. Nuclear Physics A, 2019, 982, 691-694.	1.5	0
436	Interaction of ultra-energetic cosmic neutrinos with a thermal gas of relic neutrinos. , 2007, , .	0	0
437	Probing the Extragalactic Mid-infrared Background with HAWC. Astrophysical Journal, 2022, 933, 223.	4.5	0